Optimization of Digital Overcurrent Protection Settings in DC Urban Light Railway Systems

This article has been accepted for publication in a future issue of this journal, but has not been fully edited. Content may change prior to final publication. Citation information: DOI 10.1109/TIA.2019.2914415, IEEE Transactions on Industry Applications

Optimization of Digital Overcurrent Protection Settings in DC Urban Light Railway Systems

E. Pons*, *Member, IEEE*, P. Colella*, *Member, IEEE*, R. Rizzoli† and R. Tommasini‡, *Member, IEEE*
*Politecnico di Torino - Dipartimento Energia Galileo Ferraris
Torino, 10129, ITALY
Email: enrico.pons@polito.it
†Infratrasporti.To Srl
Torino, 10122, ITALY
Email: Roberto.Rizzoli@infrato.it
‡Prof. Tommasini passed away on January 20th, 2017

***Abstract*—DC urban light railway systems are used for public transportation in many towns worldwide. In these systems, short circuit currents are often similar, both in steady state magnitude and in rate-of-rise, to normal operation currents. In order to properly set the protection relays, to obtain short circuit discrimination and to avoid nuisance trippings, it is important to analyze short circuit and normal operation current patterns. It is also important to highlight that normal operation current patterns are not only those related to rolling stock acceleration, but also to zone commutation. This paper presents the results of several measurement campaigns, performed for this purpose, on the tram network of Turin, Italy. The measurements results are then used to propose optimized settings for the installed overcurrent protections.**

I. Introduction

Light railway systems are used as public transportation systems in many towns worldwide. For these systems widely different DC voltage supply levels are used [1]. The Traction Electrification System (TES) is normally fed by power substations, which contain the power transformers, AC/DC converters, protective relays and circuit breakers. From these substations, several DC feeders (positive cables) are used to energize the Overhead Contact System (OCS). The return current is collected by the rails and by the negative cables [2].

Different types of faults can happen in DC tram networks. Close-in bolted faults (short circuits between positive and negative conductors, inside the substation or in its vicinity) give rise to very high short circuit currents. These are characterized by a high rate-of-rise di/dt in the first instants and by a high steady state magnitude. These types of fault are easily recognized by overcurrent protections and extra-rapid circuit breakers trip. Some faults, such as arcing faults (e.g. ground faults along the line) or distant bolted faults, produce smaller steady state values and rate-of-rises and are difficult to detect: both the steady state fault current magnitude and the initial rate-of-rise are in fact comparable to normal operation currents parameters [3], [4].

Traditionally, the protective relays installed in the TES power substations were instantaneous or time-delayed over-current protections, which are set to send the tripping signal to the circuit breaker when the current remains above the maximum current threshold for a certain amount of time. A thermal protection could be added for overload protection of the feeder components. Additionally, classic protective relays installed in light railway systems could have a maximum rate-of-rise threshold: in this case a tripping signal is sent to the circuit breaker also when the current rate-of-rise exceeds a defined value [3], [4]. However, due to the previously described reasons, the instantaneous and time-delayed over-current protections are not sufficient and the rate-of-rise protection of more recent relays is quite difficult to be properly set in order to obtain short-circuit discrimination and to avoid nuisance tripping.

The application guide EN 50123-7-1 (Measurement, control and protection devices for specific use in d.c. traction systems) specifies that, in particular in light-rail systems with overhead contact lines, special attention should be paid to the requirements for protection against indirect contacts. The rate-of-rise relay would satisfy this need, but the application guide itself reports that the setting is not always easy and recommends field trials to show that it will trip for the most distant fault condition [5].

In case the fault is not recognized by protective relays, and circuit breakers do not trip, risk of electric shock can be present both inside the feeding substations (where only the company employees have access) and along the tram lines (accessible to the public). Dangerous voltages can in fact be present on the rails and on extraneous conductive parts inside the substation when fault currents are circulating [2].

In previous works the authors studied ground faults inside the substation and along the line, developing appropriate steady state models for the different elements which constitute the TES [2], [6]. The results of these studies show that there are conditions in which dangerous voltages can be present on accessible metallic parts but standard over-current protections do not recognize the fault.

A first possibility that can be exploited in order to improve short circuit discrimination is to use rate-of-rise over-current protections. In [3] the optimization of the protection settings is presented. It used real operation recordings in a representative feeder for the settings improvement based on empirical data.

This article has been accepted for publication in a future issue of this journal, but has not been fully edited. Content may change prior to final publication. Citation information: DOI 10.1109/TIA.2019.2914415, IEEE Transactions on Industry Applications

Nevertheless, as previously mentioned, also the simple rate-of-rise protection can be difficult to be properly set. In fact, besides tram acceleration di/dt, much higher current derivatives can be observed when a vehicle crosses the boundary between two different zones of the OCS. The contact system, in fact, is normally divided in zones, fed by different feeders and protected by different circuit breakers. In tram networks, usually, the different zones are separated by a short insulating section or by a short element in which the two conductors run parallel to each other. In railways instead, normally, the commutation between two zones is guaranteed by a 40-50 m long section, where the power supply to the trains is provided at the same time by both contact wires, insulated each other, that run parallel at about 40 cm distance. In all of these cases, with small differences associated to the different geometry of the commutation system, when the vehicle pantograph leaves completely the old zone entering the new one, high current gradients are observed. This phenomenon is very well explained, for railway systems, in [7].

More sophisticated protection systems use a combination of current gradient di/dt, current increment ΔI and delay duration ΔT for short circuit discrimination [1]. The feeder protection relays installed in the tram network in Turin, in particular, have four different trip modes: an instantaneous or time-delayed over-current threshold, **I>**, a maximum instantaneous rate-of-rise threshold, **di>**, a maximum current increment threshold, **DR>** and a maximum steady state forecasted current threshold **EXP**. The relay logic, for having these four trip modes working properly, requires the correct setting of seven parameters.

In order to properly set these protection systems, a good knowledge of normal operation and short circuit currents patterns is required. For this purpose, the authors performed large measurement campaigns on the tram network in Turin, in Northern Italy, analysing normal operation and short circuit currents parameters [8].

In this paper the results of the measurements campaigns are presented. The current patterns in normal operation and in case of short circuit are then analyzed. The logic of the feeder protection relays installed in the tram network in Turin is described and, finally, optimized settings for these relays are proposed.

The rest of the paper is organized as follows: section II presents the results of short circuit tests; section III presents the results of a measurement campaign on tram acceleration currents; section IV presents the current patterns for the zone commutation phenomenon; in section V the different patterns are compared and the results are discussed. Then, in section VI, the new optimized settings for the protection relays are presented and discussed. Finally, some conclusions are given.

II. Short Circuit Currents

Short circuit currents in DC systems fed by rectifiers can be, for our purposes, approximated to an exponential with an overshoot that depends mainly on the DC side impedance [9]–[11]. For the cases we are mostly interested in, i.e. arcing faults or distant bolted faults, the DC side impedance is high and the overshoot is not present. The relevant parameters that must be kept into account are:

- the steady-state current magnitude I_0;
- the initial rate-of-rise of the current $\frac{di_0}{dt}$.

In the traction system where the measurement campaigns have been carried out, the AC/DC converters are constituted by 12-pulse rectifiers. Therefore the relevant values can be calculated (with some approximations, due for example to impedance variation during the fault [12]) as presented in eq. 1 and eq. 2 [9]:

$$I_0 = \frac{2 \cdot U_{d0}}{\sqrt{3} \cdot \sqrt{(R_{AC} + R_{DC})^2 + \omega^2 \cdot L_{AC}^2}} \tag{1}$$

$$\frac{di_0}{dt} = \frac{U_{d0}}{L_{AC} + L_{DC}} \tag{2}$$

where:

- U_{d0} is the rectifier no load voltage;
- R_{AC} is the AC side resistance, which is mainly constituted by the transformer windings resistances;
- R_{DC} is the DC side resistance, which is mainly constituted by the resistance of feeder cables, OCS, rails and return conductors;
- ω is the AC system frequency;
- L_{AC} is the AC side inductance, which is mainly constituted by the transformer windings inductances;
- L_{DC} is DC side inductance.

Different measurement campaigns have been performed in order to study real short circuit currents. Test short circuits have been performed both in the substations and along the lines, with or without a series additional resistance to limit the short circuit current magnitude. The measurements have been performed with a high speed digital recorder. The voltage drop on a shunt resistance was measured.

An example of the recorded waveform for a bolted fault far from the feeding substation is presented in Fig. 1. In the same figure the rate-of-rise is also reported. In this case the extra-rapid circuit breaker in the substation tripped, and so the short circuit current could not reach its steady state value I_0.

The results presented in Fig. 1 are obtained from real measurements during short circuit tests on a feeder of the tram network in Turin. The short circuit was obtained by connecting the overhead contact line to the rail with a 6 meters long $150mm^2$ cable. This was done in the worst possible location, i.e. the farthest from the power substation. Due to the transformer, rectifier, cables and overhead contact line impedances the short circuit current for this distant bolted fault reaches only about 62 A/ms.

The equations presented (eq. 1 and eq. 2) can be useful to determine the approximate line parameters from real measurements and to extend the measurement results for faults in different positions along the line or with different series impedance.

In Fig. 2 and Fig. 3 the cumulative distribution functions (cdf) of the current increment and current rate-of-rise are reported, respectively, for short circuit currents recorded during the measurements campaign. The cdf for the experimental data

This article has been accepted for publication in a future issue of this journal, but has not been fully edited. Content may change prior to final publication. Citation information: DOI 10.1109/TIA.2019.2914415, IEEE Transactions on Industry Applications

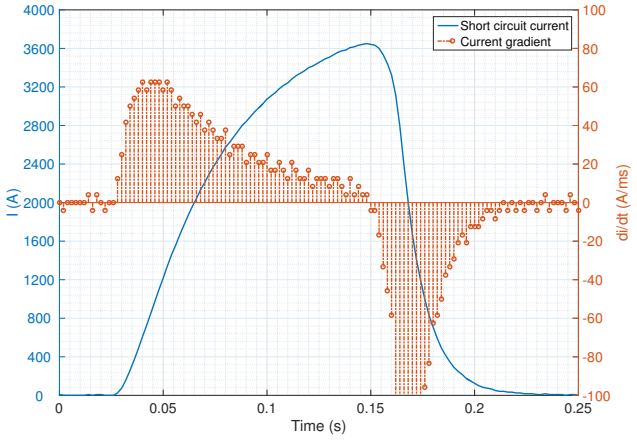

Fig. 1. Short circuit current for distant bolted fault.

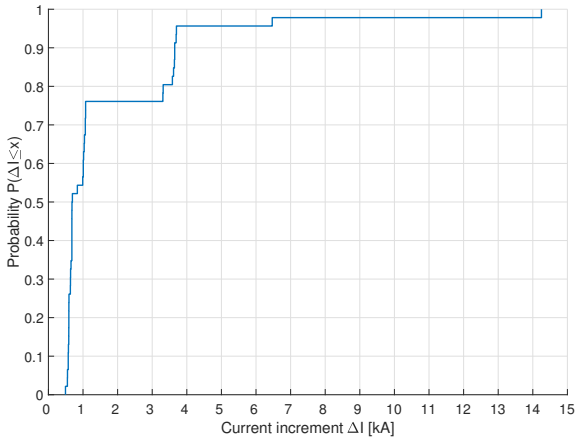

Fig. 2. Cumulative distribution function (cdf) of current increment for short circuit currents.

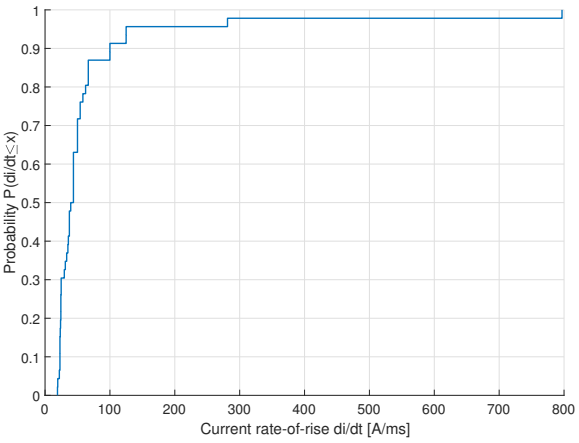

Fig. 3. Cumulative distribution function (cdf) of current rate-of-rise for short circuit currents.

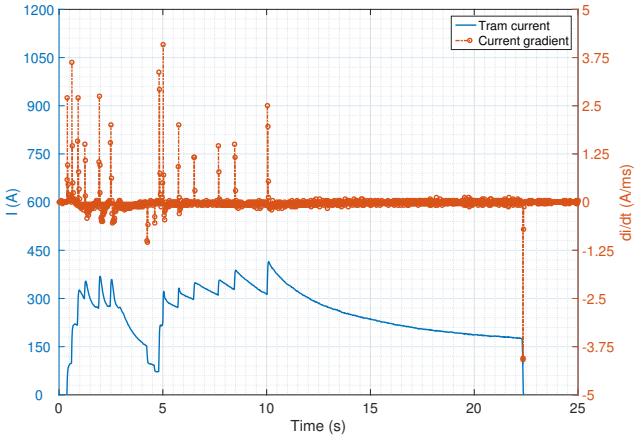

Fig. 4. Tram acceleration currents - old variable speed drive with rheostatic control.

in a vector X is defined as the probability that X will take a value less than or equal to x. Fig. 2 and Fig. 3 show therefore the probability that a short circuit will have a ΔI or a di/dt lower than a certain threshold.

The variation range for these two important parameters, for short circuit currents, is rather wide, in fact, 20 $A/ms \leq di/dt \leq 800$ A/ms and 500 $A \leq \Delta I \leq 14500$ A.

For the measurement of the short circuit currents, an opto-isolator was used to keep separate the recorder from the voltage of the system where the shunt was installed (600 V DC). It was discovered afterwards that the opto-isolator used was introducing a low-pass filter effect to the measured current waveforms. The opto-isolator was tested in laboratory to determine the low-pass filter parameters. The transfer function $H(s)$ of the equivalent filter is presented in eq. 3.

$$H(s) = \frac{1}{1+\tau s} = \frac{1}{1+0.0114s} \tag{3}$$

where τ is the time constant of the filter, corresponding to a cutoff frequency $f_0 = 14Hz$.

This effect of the opto-isolator is slightly reducing the di/dt values calculated for short circuit currents. The reduction however is negligible, is stronger on the fast short circuits, and is on the side of safety, as the protection settings will be chosen to detect short circuit less steep than the real ones.

III. Tram Acceleration Currents

Tram acceleration currents have stochastic patterns that depend on the road traffic conditions and on the driver operations. Typical acceleration currents however are related to the type of drive adopted by the vehicles. In Fig. 4 the typical current profile absorbed by an old vehicle equipped with DC motors and rheostatic control is presented. Vice-versa, in Fig. 5, the typical current profile of a modern vehicle with induction motors and variable frequency drives is showed. Also in this case the measurements have been carried out using a high speed digital recorder. It was located inside a power substation and connected to the shunt resistance on the feeder of the zone where the vehicles under test were circulating. Typical gradients are in the range from 1 A/ms to 5 A/ms.

This article has been accepted for publication in a future issue of this journal, but has not been fully edited. Content may change prior to final publication. Citation information: DOI 10.1109/TIA.2019.2914415, IEEE Transactions on Industry Applications

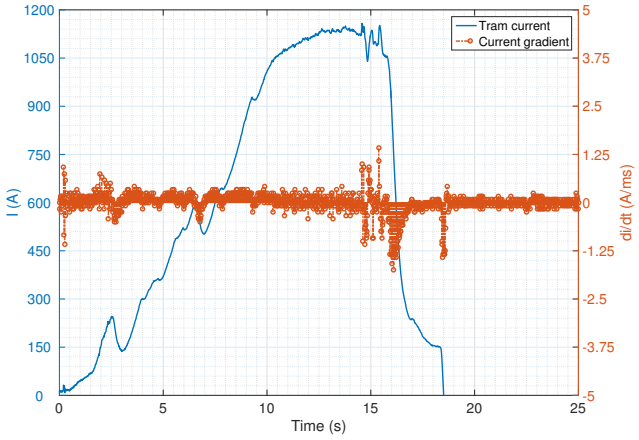

Fig. 5. Tram acceleration currents - modern variable frequency drive.

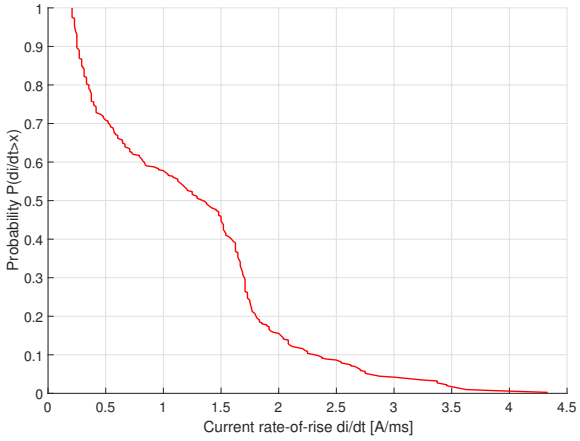

Fig. 7. Cumulative distribution function (cdf) of current rate-of-rise for tram acceleration currents.

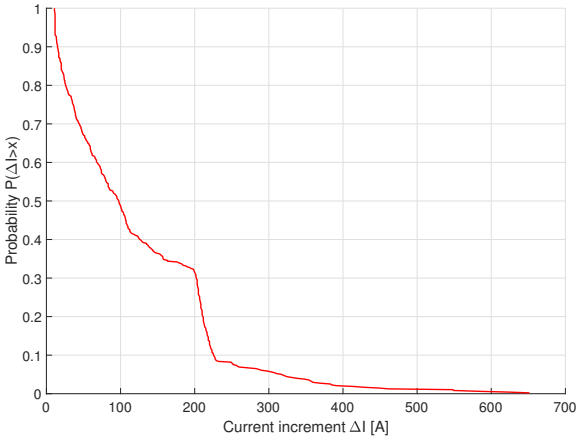

Fig. 6. Cumulative distribution function (cdf) of current increment for tram acceleration currents.

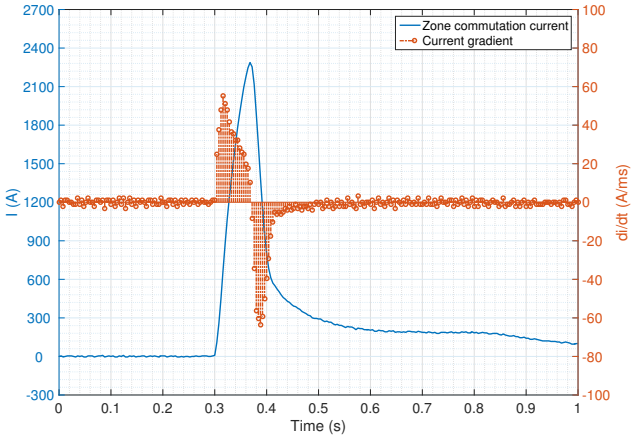

Fig. 8. Zone commutation current - vehicle with variable frequency drive.

In Fig. 6 and Fig. 7 the complementary cumulative distribution functions (ccdf) of the current increment and current rate-of-rise are reported, respectively, for tram acceleration currents, including all types of vehicles that can circulate in the tram network in Turin. The ccdf shows how often the random variable is above a particular level, so, in this case, the probability that a tram acceleration current will have a ΔI or a di/dt higher than a certain threshold.

In this case, the variation range for the two parameters is much smaller, as $0.2\ A/ms \leq di/dt \leq 4.3\ A/ms$ and $10\ A \leq \Delta I \leq 650\ A$.

IV. Zone Commutation Currents

As previously mentioned, besides tram acceleration di/dt and ΔI, much higher current derivatives and increments can be observed when a vehicle crosses the boundary between two different zones of the OCS. In Fig. 8, as an example, the current absorbed when a modern vehicle equipped with induction motors and variable frequency drives enters the new zone is presented.

By comparing the gradients presented in Fig. 1 for the short circuit and Fig. 8 for the zone commutation, it is immediately evident that comparable values of rate-of-rise can be reached, in this example close to 80 A/ms.

Other types of vehicles produce different current patterns when they cross the boundary between two different zones of the OCS.

In Fig. 9 and Fig. 10 two additional examples are presented. They are both recorded when a vehicle equipped with a chopper speed controller crosses the boundary between two zones. In the first case, the vehicle speed is high, the time required to cross the insulating element is low, and the electronics does not reset. In the second case, vice versa, the vehicle speed is low, the time required to cross the insulating element is high, and the electronics resets.

In both cases very high current rates-of rise are recorded. The interesting point, however, is that the current starts decreasing after a short period of time, lower than 0.1 s.

For these cases, the measurements have been carried out installing the high speed digital recorder on board of the vehicle and positioning a current clamp on the vehicle imperial, where

This article has been accepted for publication in a future issue of this journal, but has not been fully edited. Content may change prior to final publication. Citation information: DOI 10.1109/TIA.2019.2914415, IEEE Transactions on Industry Applications

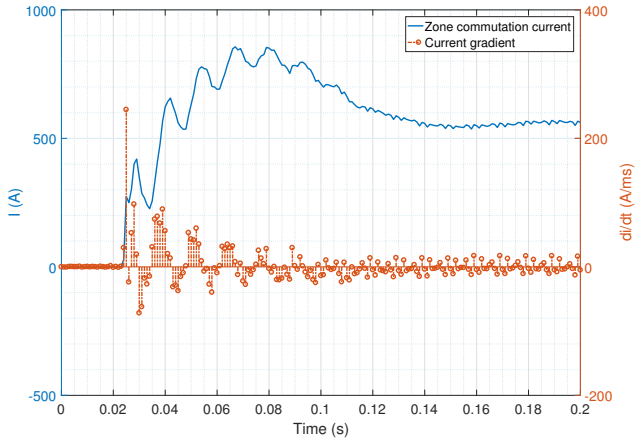

Fig. 9. Zone commutation current - vehicle with chopper (A).

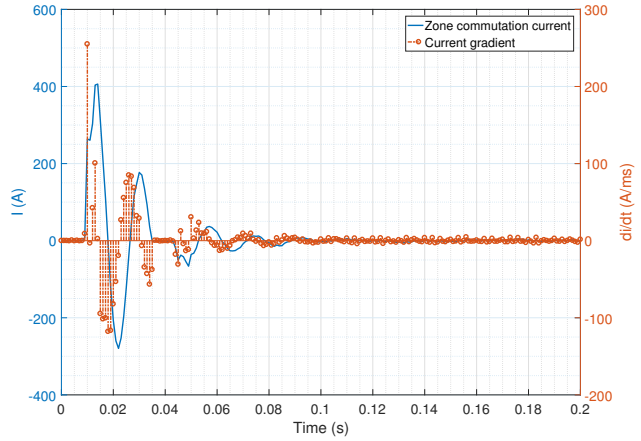

Fig. 10. Zone commutation current - vehicle with chopper (B).

the power cables receive the current from the pantograph.

In Fig. 11 and Fig. 12 the complementary cumulative distribution functions of the current increment and current rate-of-rise are reported, respectively, for zone commutation currents.

In both figures the ccdf for vehicles equipped with variable frequency drive and chopper are compared. It can be observed that variable frequency drives can generate much higher current increments ΔI, but lower current rates-of-rise di/dt.

In the case of zone commutation currents it is particularly interesting to analyze the variation range of the two parameters, as this can be compared with the variation range for short circuit currents.

For zone commutation currents the variation range is again quite large, as $1\ A/ms \leq di/dt \leq 300\ A/ms$ and $100\ A \leq \Delta I \leq 2300\ A$.

V. Normal Operation and Short Circuit Comparison

Once the current patterns, for the different possible cases related to normal operation and short circuit, have been individually studied, it is interesting to make a comprehensive

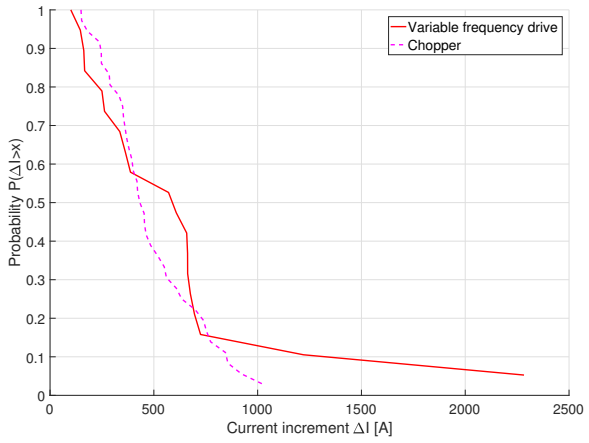

Fig. 11. Cumulative distribution function (cdf) of current increment for zone commutation currents.

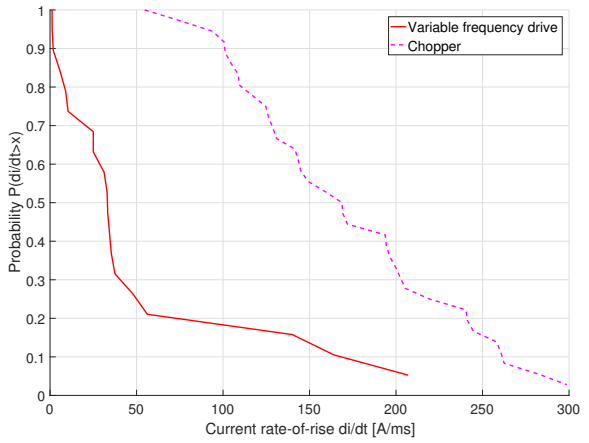

Fig. 12. Cumulative distribution function (cdf) of current rate-of-rise for zone commutation currents.

analysis. For this purpose the current patterns have been grouped in normal currents (including acceleration and zone commutation currents) and short circuit currents. An overall ccdf has been calculated for normal operation currents, that can be compared, in the same plot, with the cdf of short circuit currents. In Fig. 13 the comparison is performed for the current increment ΔI, while in Fig. 14 for the rate-of-rise di/dt. A logarithmic scale is used for current increment and rate-of-rise to improve comprehension, because the variation ranges are different.

The presented plots show that there is a range of values clearly related to fault conditions and a range of values clearly related to normal operations. However, there is also a range of values, for both ΔI and di/dt, in which fault conditions and normal operation are overlapped.

The setting of the protection relays, in terms of current increment and rate-of-rise, should be a compromise between fault discrimination and nuisance tripping.

Plots similar to those presented in Fig. 13 and Fig. 14 could be therefore used to evaluate, for a certain proposed setting

This article has been accepted for publication in a future issue of this journal, but has not been fully edited. Content may change prior to final publication. Citation information: DOI 10.1109/TIA.2019.2914415, IEEE Transactions on Industry Applications

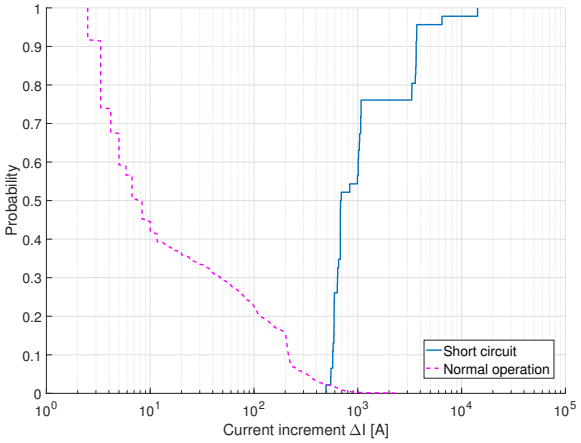

Fig. 13. Cumulative distribution function (cdf) of current increment comparison.

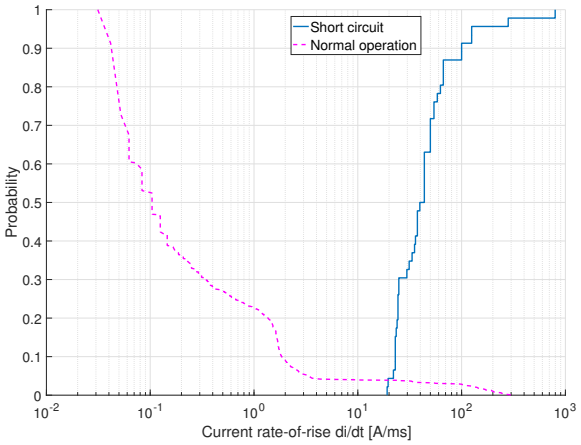

Fig. 14. Cumulative distribution function (cdf) of current rate-of-rise comparison.

of the relay, the probability of having nuisance tripping and the probability of missing the detection of certain fault events characterized by a high impedance.

The plots presented in this paper in Fig. 13 and Fig. 14 can provide only qualitative indications and not accurate information on the probabilities. In fact, they have been constructed by putting together all the data acquired during the measurement campaigns, but the number of available measurements for the different vehicle types, for acceleration and zone commutation currents and for short circuit tests were not the same.

VI. Protection Settings Optimization

The digital relays installed in the tram network in Turin work with the following logic (in the square brackets the parameters to be set):

- the current i is measured with a sampling time of $2ms$;
- if $i > [I >]$ the relay sends a trip command **I>**;
- every $2ms$, the relay calculates the current rate-of-rise in A/ms as $\Delta i/\Delta t = (i_j - i_{j-1})/2$;

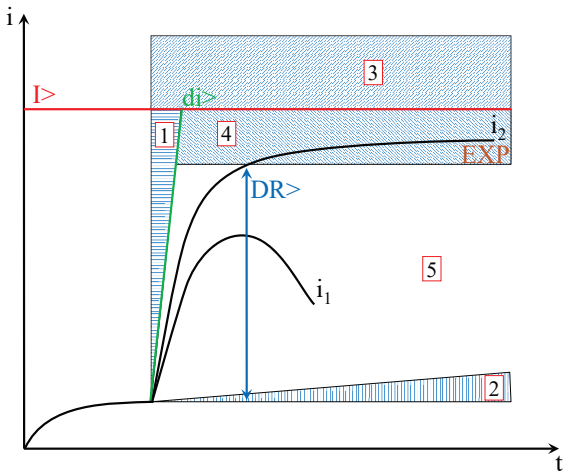

Fig. 15. Digital relay operation areas.

- if $\Delta i/\Delta t > [A/msD]$ the relay recognizes an event and starts the monitoring cycle, in which the current pattern is monitored for a period of time $t_n = 2[iEn]ms$:
  - the initial current I_0 is stored in the memory;
  - every $2ms$, the relay calculates the current rate-of-rise in A/ms as $\Delta i/\Delta t = (i_j - i_{j-1})/2$;
  - every $2ms$, the relay calculates the current increment $\Delta I = i_j - I_0$;
  - if $\Delta i/\Delta t > [A/ms >]$ the relay sends a trip command **di>**;
  - if $\Delta i/\Delta t < [A/msE]$ the relay exits from the monitoring cycle and resets;
  - if $\Delta I > [DR >]$ the relay sends a trip command **DR>**;
- At the time t_n, if there was nor a reset neither a trip command, the relay calculates the steady-state value DRc of the current, starting from I_0, with the hypothesis of exponential waveform with time constant $\tau = 2[iEn]ms$: $DRc = (i_n - I_0)/0.632$;
- if $DRc > [DR >]$ the relay sends a trip command **EXP**;
- if $DRc < 0.5[DR >]$ the relay exits from the monitoring cycle and resets;
- if $0.5[DR >] < DRc < [DR >]$ the monitoring cycle is extended of $t = \dfrac{[tEx] \cdot [DR >]}{DRc}$ with the same logic described before;

Summing up, the protection relay has four different trip modes: **I>**, **di>**, **DR>** and **EXP**, which are graphically presented in Fig. 15. In this figure, in particular: the current i_1 is an example of acceleration current; the current i_2 is an example of short circuit current; in area 1 the relay trips for maximum rate-of-rise; in area 2 the relay never trips and does not start the transient analysis; in area 3 the relay trips for maximum total current; in area 4 the relay can trip for maximum current increment or EXP; in area 5 the relay is analyzing the transient.

The settings to be chosen and optimized for the proper operation of the four trip modes are: $[I >]$, $[A/msD]$, $[A/ms >]$, $[A/msE]$, $[DR >]$, $[iEn]$ and $[tEx]$. Their choice

This article has been accepted for publication in a future issue of this journal, but has not been fully edited. Content may change prior to final publication. Citation information: DOI 10.1109/TIA.2019.2914415, IEEE Transactions on Industry Applications

will be discussed in the following paragraphs.

A. Maximum Current $[I >]$

The maximum current threshold $[I >]$ is mainly devoted to protection against cable overload. This setting is not useful for discrimination between normal operation and short circuit. This setting depends on the cables installed in the network. In Turin, depending on the considered zone, it is set in the range from $3600A$ to $4100A$.

B. Event Recognition Threshold $[A/msD]$

The first important threshold is the event recognition threshold $[A/msD]$. This threshold must be set in such a way to be sure that for all possible short circuit events it will be triggered and the relay will enter into the monitoring cycle. The minimum rate-of-rise measured in short circuits without series resistances, for a distant bolted fault, was of $42A/ms$. To keep a safety margin the event recognition threshold was set as $[A/msD] = 30A/ms$.

C. Maximum Rate-of-rise $[A/ms >]$

The maximum rate-of-rise threshold $[A/ms >]$ must answer two opposing needs: a greater value reduces the possibility of nuisance trippings due to zone commutation currents; on the contrary, a smaller value guarantees a faster tripping in case of short circuit. In any case, this threshold will play an important role only for close-in bolted faults, enabling a limitation action of the circuit breaker. This parameter is not useful to detect and recognize distant bolted faults. In order to avoid as much as possible nuisance trippings, it was chosen $[A/ms >] = 120A/ms$. It can be seen from Fig. 14 that only a small tail of the cdf for normal operation exceeds this value.

D. Monitoring Cycle Duration $[iEn]$

As explained at the beginning of Section VI, the hypothesis at the basis of the relay logic is to perform certain calculations after a time t_n corresponding to the time constant of the slowest and farthest short circuit. This time constant was calculated and corresponds to $36ms$. For this reason it was chosen $[iEn] = 18$.

E. Reset Threshold $[A/msE]$

The reset threshold must be chosen in such a way that, for the farthest and slowest short circuit, the relay will not reset before time t_n. The setting of $[A/msE]$ must therefore be smaller than the rate of rise of the farthest and slowest short circuit at t_n. The calculated rate of rise for this type of short circuit at $t_n = \tau$ was $di/dt = 17A/ms$. For this reason, to keep a safety margin, it was chosen $[A/msE] = 10A/ms$.

F. Maximum Current Increment $[DR >]$

The maximum current increment $[DR >]$ is the fundamental parameter in the recognition of distant short circuits, characterized by low rates-of-rise. The proposed setting is based on the maximum value of current increment recorded under ordinary conditions, corresponding to the worst zone commutation case (see Fig. 11). Values of this entity are rarely found in normal operation, but in any case they must not be exchanged for short circuits. It was therefore chosen $[DR >] = 2400A$.

G. Monitoring Cycle Extension $[tEx]$

The duration of the short circuit phenomena is very short. After an amount of time $t = 5\tau$ the exponential short circuit has reached its steady state. The monitoring cycle extension time was therefore set at its minimum allowed value as $[tEx] = 1s$

VII. Conclusion

The problem of short circuit discrimination in DC urban light railway systems is studied in this paper. The final goal is the optimization of the settings of the feeder protection relays installed in the tram network in Turin. For this purpose, several measurements campaigns have been performed. In particular, currents related to tram acceleration, zone commutation and short circuits have been considered. The results of the campaigns have been presented and discussed, also resorting to a statistical analysis and to the presentation of cumulative distribution functions and complementary distribution functions.

The results show that there is a range of values clearly related to fault conditions and a range of values clearly related to normal operations. However, there is also a range of values, for both current increment and rate-of-rise, in which fault conditions and normal operation are overlapped.

For this reason the setting of the protection relays is a compromise between fault discrimination and nuisance tripping. In this paper an optimized set of settings is proposed.

In conclusion it can be said that, due to the problem of zone commutation currents, the maximum rate-of-rise threshold cannot be used for distant short circuit discrimination but only for accelerating the circuit breaker tripping for close-in bolted faults. This type of fault, however, would have been detected after a longer time also by traditional overcurrent protections. The most promising parameter for distant short circuit discrimination is instead the maximum current increment threshold. Nevertheless, some distant arcing faults may still remain undetected.

Acknowledgment

The authors would like to thank the personnel of GTT and Infra.To for their valuable support in this research.

References

[1] M. Li, J. He, Z. Bo, H. Yip, L. Yu, and A. Klimek, "Simulation and algorithm development of protection scheme in dc traction system," in *PowerTech, 2009 IEEE Bucharest*. IEEE, 2009, pp. 1–6.

[2] E. Pons, R. Tommasini, and P. Colella, "Electrical safety of dc urban rail traction systems," in *Environment and Electrical Engineering (EEEIC), 2016 IEEE 16th International Conference on*. IEEE, 2016, pp. 1–6.

[3] M. Reis, "Optimization of dc feeder rate of rise overcurrent protection settings using delta i cumulative distribution," in *Industrial and Commercial Power Systems Technical Conference, 2004 IEEE*. IEEE, 2004, pp. 63–66.

[4] J. S. Morton, "Circuit breaker and protection requirements for dc switchgear used in rapid transit systems," *IEEE transactions on industry applications*, no. 5, pp. 1268–1273, 1985.

[5] *Railway applications - Fixed installations - D.C. switchgear Part 7-1: Measurement, control and protection devices for specific use in d.c. traction systems - Application guide*. Standard EN 50123-7-1, 2003.

[6] E. Pons, R. Tommasini, and P. Colella, "Fault current detection and dangerous voltages in dc urban rail traction systems," *IEEE Transactions on Industry Applications*, vol. 53, no. 4, pp. 4109–4115, 2017.

[7] E. Cinieri, A. Fumi, V. Salvatori, and C. Spalvieri, "A new high-speed digital relay protection of the 3-kvdc electric railway lines," *Power Delivery, IEEE Transactions on*, vol. 22, no. 4, pp. 2262–2270, 2007.

[8] E. Pons, P. Colella, R. Rizzoli, and R. Tommasini, "Distinguishing short circuit and normal operation currents in dc urban light railway systems," in *Environment and Electrical Engineering and 2017 IEEE Industrial and Commercial Power Systems Europe (EEEIC/I&CPS Europe), 2017 IEEE International Conference on*. IEEE, 2017, pp. 1–6.

[9] C. Pires, S. Nabeta, and J. R. Cardoso, "Second-order model for remote and close-up short-circuit faults currents on dc traction supply," *IET Power Electronics*, vol. 1, no. 3, pp. 348–355, 2008.

[10] P. Pozzobon, "Transient and steady-state short-circuit currents in rectifiers for dc traction supply," *Vehicular Technology, IEEE Transactions on*, vol. 47, no. 4, pp. 1390–1404, 1998.

[11] M. Berger, C. Lavertu, I. Kocar, and J. Mahseredjian, "Performance analysis of dc primary power protection in railway cars using a transient analysis tool," in *Vehicle Power and Propulsion Conference (VPPC), 2015 IEEE*. IEEE, 2015, pp. 1–7.

[12] J. Brown, J. Allan, and B. Mellitt, "Calculation of remote short circuit fault currents for dc railways," in *IEE Proceedings B (Electric Power Applications)*, vol. 139, no. 4. IET, 1992, pp. 289–294.